



# East Asian Monsoonal Climate Sensitivity Changed in the Late Pliocene in Response to Northern Hemisphere Glaciations

Ze Zhang, Alexis Licht, David de Vleeschouwer, Zhixiang Wang, Yanzhen Li, David B Kemp, Liangcheng Tan, Rui Zhang, Xiaoke Qiang, Chunju Huang

## ► To cite this version:

Ze Zhang, Alexis Licht, David de Vleeschouwer, Zhixiang Wang, Yanzhen Li, et al.. East Asian Monsoonal Climate Sensitivity Changed in the Late Pliocene in Response to Northern Hemisphere Glaciations. *Geophysical Research Letters*, 2022, 49, 10.1029/2022gl101280 . hal-03894632

HAL Id: hal-03894632

<https://hal.science/hal-03894632>

Submitted on 12 Dec 2022

**HAL** is a multi-disciplinary open access archive for the deposit and dissemination of scientific research documents, whether they are published or not. The documents may come from teaching and research institutions in France or abroad, or from public or private research centers.

L'archive ouverte pluridisciplinaire **HAL**, est destinée au dépôt et à la diffusion de documents scientifiques de niveau recherche, publiés ou non, émanant des établissements d'enseignement et de recherche français ou étrangers, des laboratoires publics ou privés.



Distributed under a Creative Commons Attribution - NonCommercial - NoDerivatives 4.0 International License

# Geophysical Research Letters®

## RESEARCH LETTER

10.1029/2022GL101280

### Key Points:

- Cyclic patterns in East Asian summer monsoonal intensity during the Pliocene were mainly driven by Antarctic ice sheet variations
- A major reorganization of the East Asian climate system occurred at 2.75–2.6 Ma in response to Northern Hemisphere glaciation
- Quaternary East Asian summer monsoon on orbital scales displays a sensitivity that is unique to the modern icehouse with bipolar ice sheets

### Supporting Information:

Supporting Information may be found in the online version of this article.

### Correspondence to:

Z. Wang and C. Huang,  
[wangzhi8905@126.com](mailto:wangzhi8905@126.com);  
[huangcj@cug.edu.cn](mailto:huangcj@cug.edu.cn)

### Citation:

Zhang, Z., Licht, A., De Vleeschouwer, D., Wang, Z., Li, Y., Kemp, D. B., et al. (2022). East Asian monsoonal climate sensitivity changed in the late Pliocene in response to Northern Hemisphere glaciations. *Geophysical Research Letters*, 49, e2022GL101280. <https://doi.org/10.1029/2022GL101280>

Received 14 SEP 2022  
Accepted 22 NOV 2022

### Author Contributions:

**Conceptualization:** Ze Zhang, Alexis Licht, Zhixiang Wang, Chunju Huang  
**Data curation:** Alexis Licht, David De Vleeschouwer, David B. Kemp, Xiaoke Qiang, Chunju Huang  
**Formal analysis:** Ze Zhang, Alexis Licht, Yanzhen Li, David B. Kemp, Liangcheng Tan, Rui Zhang  
**Funding acquisition:** Zhixiang Wang, Chunju Huang

© 2022. The Authors.  
This is an open access article under the terms of the Creative Commons Attribution-NonCommercial-NoDerivs License, which permits use and distribution in any medium, provided the original work is properly cited, the use is non-commercial and no modifications or adaptations are made.

## East Asian Monsoonal Climate Sensitivity Changed in the Late Pliocene in Response to Northern Hemisphere Glaciations

Ze Zhang<sup>1</sup>, Alexis Licht<sup>2</sup> , David De Vleeschouwer<sup>3</sup> , Zhixiang Wang<sup>4</sup> , Yanzhen Li<sup>1,5</sup>, David B. Kemp<sup>1</sup> , Liangcheng Tan<sup>5,6,7</sup> , Rui Zhang<sup>8</sup>, Xiaoke Qiang<sup>5</sup> , and Chunju Huang<sup>1</sup> 

<sup>1</sup>State Key Laboratory of Biogeology and Environmental Geology, Hubei Key Laboratory of Critical Zone Evolution, School of Earth Sciences, China University of Geosciences, Wuhan, China, <sup>2</sup>CEREGE, Aix Marseille University, CNRS, IRD, INRAE, Aix-en-Provence, France, <sup>3</sup>Institute of Geology and Paleontology, University of Münster, Münster, Germany, <sup>4</sup>Qinghai Provincial Key Laboratory of Geology and Environment of Salt Lakes, Qinghai Institute of Salt Lakes, Chinese Academy of Sciences, Xining, China, <sup>5</sup>State Key Laboratory of Loess and Quaternary Geology, Institute of Earth Environment, Chinese Academy of Sciences, Xi'an, China, <sup>6</sup>Open Studio for Oceanic Continental Climate and Environment Changes, Pilot National Laboratory for Marine Science and Technology (Qingdao), Qingdao, China, <sup>7</sup>Institute of Global Environmental Change, Xi'an Jiaotong University, Xi'an, China, <sup>8</sup>College of Urban and Environmental Sciences, Hubei Normal University, Huangshi, China

**Abstract** Mio-Pliocene sedimentary archives of the East Asian summer monsoon (EASM) in NE Tibet record a monotonic response to orbital forcing, dominated by eccentricity. By contrast, Pleistocene archives display a more stochastic response that varies regionally and temporally. When and why this response changed is poorly understood. Here, we present a new high-resolution Rb/Sr ratio data set of EASM intensity from the Sanmenxia Basin, North China, that spans the Plio-Pleistocene transition. Our results indicate decreased monsoonal rainfall in the late Pliocene, dated at 2.75–2.6 Ma, associated with an intensified response to obliquity and enhanced climate stochasticity. This transition is attributed to the increase of Northern Hemisphere ice volume. Quaternary monsoons display a sensitivity unique to the modern icehouse with large bipolar ice sheets, while pre-Quaternary monsoons were solely impacted by Antarctic ice sheet dynamics on orbital time-scales.

**Plain Language Summary** The late Pliocene-early Pleistocene transition (LP/EP) is a period of global cooling and the intensification of Northern Hemisphere glaciation. Yet, the evolution of the East Asian summer monsoon (EASM) during this time remains a topic of ongoing discussion and debate. Here we present high-resolution paleoclimate data from a record of lake sediments across the Pliocene-Pleistocene transition period. We show that there was a reorganization of the East Asian monsoon system 2.75–2.6 million years ago, associated with an increase in climate forcing caused by cyclic changes in Earth's tilt and in climate stochasticity. This transition is attributed to the appearance of new high-latitude forcing mechanisms on monsoon intensity caused by the growth of ice sheets in the Northern Hemisphere.

## 1. Introduction

Reconstructing monsoon variability during past Greenhouse periods is critical for understanding its future response(s) to global warming. The East Asian Summer Monsoon (EASM) is a critical component of the Asian monsoonal system and brings abundant moisture from the Pacific Ocean and the South China Sea to East Asia (J. B. Liu et al., 2015; J. Y. Lu et al., 2021; Z. X. Wang et al., 2019, 2021). On orbital time-scales (ca. 10–100 kyr), EASM intensity and inland penetration are sensitive to pCO<sub>2</sub> (Kripalani et al., 2007; H. Lu et al., 2013; Luo et al., 2021), as well as variations in insolation driven by Earth's astronomical configuration (Ao, Dupont-Nivet, et al., 2020; Sun, Kutzbach, et al., 2015; Y. C. Wang et al., 2020). Recent studies demonstrate that EASM sensitivity to astronomical forcing changed with time, following mechanisms that remain poorly understood (Sun, Kutzbach, et al., 2015; Y. C. Wang et al., 2020).

Sensitivity of EASM precipitation to astronomical forcing is well-documented in paleosols and records of past lake expansion/contraction in lacustrine basins of North China (Sun, Kutzbach, et al., 2015; Y. C. Wang et al., 2020). Variations in pedogenesis and/or lake level can be reconstructed by Rb/Sr (rubidium/strontium) and other elemental ratios, for example, Al/Na and Ti/Zr, because these proxies are sensitive to the hydroclimate (Ao, Rohling, et al., 2021; Jin et al., 2020). Climate variability reconstructed using such ratios are dominated by

**Investigation:** Ze Zhang, Zhixiang Wang, Yanzhen Li, Rui Zhang

**Methodology:** Ze Zhang, Alexis Licht, David De Vleeschouwer, Zhixiang Wang, Yanzhen Li, David B. Kemp, Liangcheng Tan

**Resources:** Zhixiang Wang, Yanzhen Li, Liangcheng Tan, Xiaoke Qiang, Chunju Huang

**Software:** Ze Zhang, David De Vleeschouwer, Rui Zhang, Xiaoke Qiang, Chunju Huang

**Validation:** Ze Zhang, Alexis Licht, David De Vleeschouwer, Zhixiang Wang, Liangcheng Tan, Xiaoke Qiang, Chunju Huang

**Visualization:** Ze Zhang, David De Vleeschouwer

**Writing – original draft:** Ze Zhang

**Writing – review & editing:** Alexis Licht, David De Vleeschouwer, Zhixiang Wang, David B. Kemp, Chunju Huang

100 kyr eccentricity cycles from the mid Oligocene to the Pliocene, 28–3 Myr ago (Ao, Liebrand, et al., 2021; Ao, Rohling, et al., 2021; Nie et al., 2017; Z. X. Wang, et al., 2019, 2021). Longer-scale 405 kyr eccentricity forcing is also observed in sufficiently long records (e.g., Ao, Rohling, et al., 2021). This prominent eccentricity signature is intriguing because eccentricity has a negligible direct influence on insolation patterns. Hence, it operates through a series of non-linear processes within the carbon cycle and/or cryosphere (Ao, Liebrand, et al., 2021). Quaternary sediment archives that record EASM sensitivity to astronomical forcing yield contrasting results. Most Quaternary Chinese sedimentary basins are marked by eolian dust input, generated in central Asia and carried by winter winds (An, 2000). The study of grain-size and magnetic properties in loess deposits indicate dominant 41 kyr obliquity cycles before 0.9 Ma and 100 kyr eccentricity cycles since then (e.g., Sun, Clemens, et al., 2006, 2010). This pattern is consistent with astronomical rhythms preserved in benthic  $\delta^{18}\text{O}$  data (De Vleeschouwer et al., 2020; Lisiecki & Raymo, 2005; Westerhold et al., 2020). Other magnetic properties-based proxies suggest prominent 405-kyr eccentricity cycles (C. Y. Liu et al., 2021). In contrast, microcodium  $\delta^{18}\text{O}$  and elemental variations are dominantly forced by 41 kyr obliquity cycles over the last 1.5 Myr (T. Li et al., 2017). This discrepancy suggests that the evolution of dust transport controlled by the East Asian winter monsoon and the evolution of soil water controlled by the EASM are influenced by different processes (T. Li et al., 2017). The combination of both influences on sedimentary material yields regional and temporal complexities.

Previous work suggests that EASM intensity lost its monotonic eccentricity pacing sometime in the late Neogene, and shifted to a much more complex sensitivity to astronomical parameters, with obliquity becoming a major player during most of the Quaternary (T. Li et al., 2017; Sun, Clemens, et al., 2006, 2010). Yet, the causes and precise timing of this shift remain poorly understood. Investigating when and why this shift occurred is critical to understand the modern and future mechanisms of monsoonal intensity. The sedimentary fill of the Sanmen paleolake in the Sanmenxia Basin, North China, spans from the early Pliocene to late Pleistocene (S. B. Wang et al., 1999, 2004) and thus covers the time during which the EASM changed its response to radiative forcing. Here, we present a high-resolution (1.8 kyr) geochemical record spanning the interval from 3.9 to 2.2 Ma from the Sanmenxia Basin to decipher orbital-scale lake level changes in response to EASM variability during this key interval.

## 2. Materials and Methods

### 2.1. Sampling

The Sanmenxia Basin is a sub-basin of the larger Fenwei Basin (J. Liu et al., 2019), enclosed by the East Qinling mountains to the south, and the Zhongtiao Mountains to the north (Figure S1 in Supporting Information S1). The Sanmenxia Basin was occupied by closed lakes until the opening of the Sanmen gorge in the Mid Pleistocene (S. B. Wang et al., 1999, 2004, B. Wang et al., 2013). The Sanmen Formation is dated to the Pliocene—early Pleistocene by magnetostratigraphy and thermoluminescence dating (S. B. Wang et al., 1999).

Our sampling profile at the Huangdigou section covers the lower part of the Sanmen Formation with its diagnostic basal conglomerates and subsequent colored clays, and is capped by fluvial sands. The profile is unconformably capped by late Quaternary loess (S. B. Wang et al., 1999). Our study focuses on the lacustrine deposits beneath the Quaternary loess. These lithologies indicate an environmental shift from alluvial fans to fluvio-lacustrine alternations in a shallow, closed lake system, and finally to fluvial deposits (Text S1 in Supporting Information S1). Biostratigraphic dating based on fossil mammals and ostracods near our section indicates a Pliocene to Pleistocene age for the strata (Huang & Ji, 1984; Huang & Sun, 1959; Yuan, 1986), and this corroborates with the dating of S. B. Wang et al. (1999). The same strata have been alternatively attributed to the Mio-Pliocene (Xiao et al., 2021), though this alternative correlation provides unrealistic changes of depositional rates and is incompatible with thermoluminescence dating of the uppermost part of the section (S. B. Wang et al., 1999). It should be noted that our sampling site belongs to the same geological unit as S. B. Wang et al. (1999), but in a new area about 2 km away from their profile. Thus, the lithology and stratal thickness are slightly different (Figure S2 in Supporting Information S1). We sampled a 90 m-thick section at ca. 40 cm resolution for magnetostratigraphic dating to increase the dating precision (100 cm resolution in S. B. Wang et al., 1999; see Text S3 in Supporting Information S1 for detailed paleomagnetic analyses procedures) and sampled the central part of the section (40–81 m, where fine-grained lacustrine deposits are prominent) at 4 cm resolution for Rb/Sr analysis (see Text S2 in Supporting Information S1 for a description of climate proxies).

## 2.2. Rb/Sr

Sampling trenches were excavated to a depth of >0.5 m from the freshly exposed surfaces for sedimentary logging and sampling. The abundance of rubidium (Rb) and strontium (Sr) were measured in the field with an Innov-X Systems X-ray fluorescence spectrometer in geochemistry mode using beam 1 (50 kv) and beam 2 (10 kv). The measurement time for each sample analysis was at least 50 s. A total of 945 data points were acquired with a measurement interval of 4 cm.

## 2.3. Spectral Analysis and Cross-Spectral Analysis

Spectral analysis of the Rb/Sr data was done on the 40–81 m (corrected thickness is 40–77.6 m after removing a gravel layer between 71.6 and 75 m) interval of our section where fine-grained lacustrine deposits are prominent. The power spectra and sliding window spectral analysis of Rb/Sr in the thickness domain and time domain were calculated using Acycle 2.0 software (M. S. Li et al., 2019). Cross-spectral analysis results were generated using the “ARAND” program from Brown University, USA (Howell et al., 2006; see Text S4 in Supporting Information S1 for detailed descriptions).

# 3. Results

## 3.1. Paleomagnetic Results

The detailed magnetic polarity stratigraphy of our section is displayed on Figure 1. We identified eight normal (N1–N8) and seven reversed (R1–R7) polarity zones, based on at least two points to determine a polarity zone (Figure 1). Both the normal and reversed polarity intervals match well with all of the geomagnetic polarity time scale polarity subzones within the age interval from chron C3n to C2n (4.8–1.9 Ma). Subsequently, the age of each sampling level was estimated by piecewise linear interpolation between age control points, enabling the sediment accumulation rate of each polarity interval to be obtained.

## 3.2. Cyclostratigraphic Results

Based on the magnetostratigraphy, the fluvio-lacustrine deposits (40–81 m) in our section span a duration of ~1.7 Myr across the interval 3.9–2.2 Ma, with an average sedimentation rate of ~2.2 cm/kyr that remains broadly stable (see Text S5 in Supporting Information S1 for full details; note that the thick conglomerate interval of 71.6–75 m was removed for this calculation). This time window covers the Plio-Pleistocene transition. The sampling interval (4 cm) corresponds to a 1.8-kyr temporal sampling resolution (assuming a 2.2 cm/kyr sedimentation rate). Thus, this is sufficient to resolve individual precession, obliquity, and eccentricity cycles. Based on the sedimentation rate, the ~1,000-cm and ~270-cm cycles in the raw (thickness domain) Rb/Sr data represent ~405 and ~100 kyr eccentricity cycles, while the ~100-cm spectral peak is interpreted as a ~41 kyr obliquity signal (Figure 2c).

The 405 and 100 kyr eccentricity cycles are the dominant astronomical controls on Rb/Sr in the late Pliocene, but the dominant orbital forcing shifts to 41 kyr obliquity at the Plio-Pleistocene transition (i.e., 2.6 Ma) at ~70 m, after a 0.15 Myr transition period (2.75–2.6 Ma) with limited 100 kyr cyclicity (Figure 2). These changes occurred while accumulation rates remained unchanged (Figure 2g), corroborating the accuracy of our age model.

## 3.3. Recurrence Analysis Results

We apply a recurrence analysis measure of determinism (DET) to our record to identify individual climate states that share statistically distinctive dynamics (Steffen et al., 2018; see Text S6 in Supporting Information S1). DET values close to zero correspond to unpredictable (stochastic) climate dynamics while large values indicate deterministic dynamics. The DET parameter can thus be used to highlight climate state transitions (Westerhold et al., 2020). DET values average  $0.70 \pm 0.12$  ( $2\sigma$ ) over the interval 3.9–2.75 Ma (40–66.5 m). They then experience a marked peak over the interval 2.75–2.7 Ma (66.5–67.5 m; average =  $0.89 \pm 0.12$  ( $2\sigma$ )). DET values decrease to  $0.58 \pm 0.14$  ( $2\sigma$ ) between 2.6 and 2.2 Ma (67.5–81 m; Figure 3). This decrease broadly coincides with the timing of the orbital cyclicity shift from eccentricity to obliquity across the Plio-Pleistocene transition. A *t*-test performed on DET values confirms a higher stochasticity after 2.6 Ma than before 2.75 Ma ( $p = 0.027$ ).

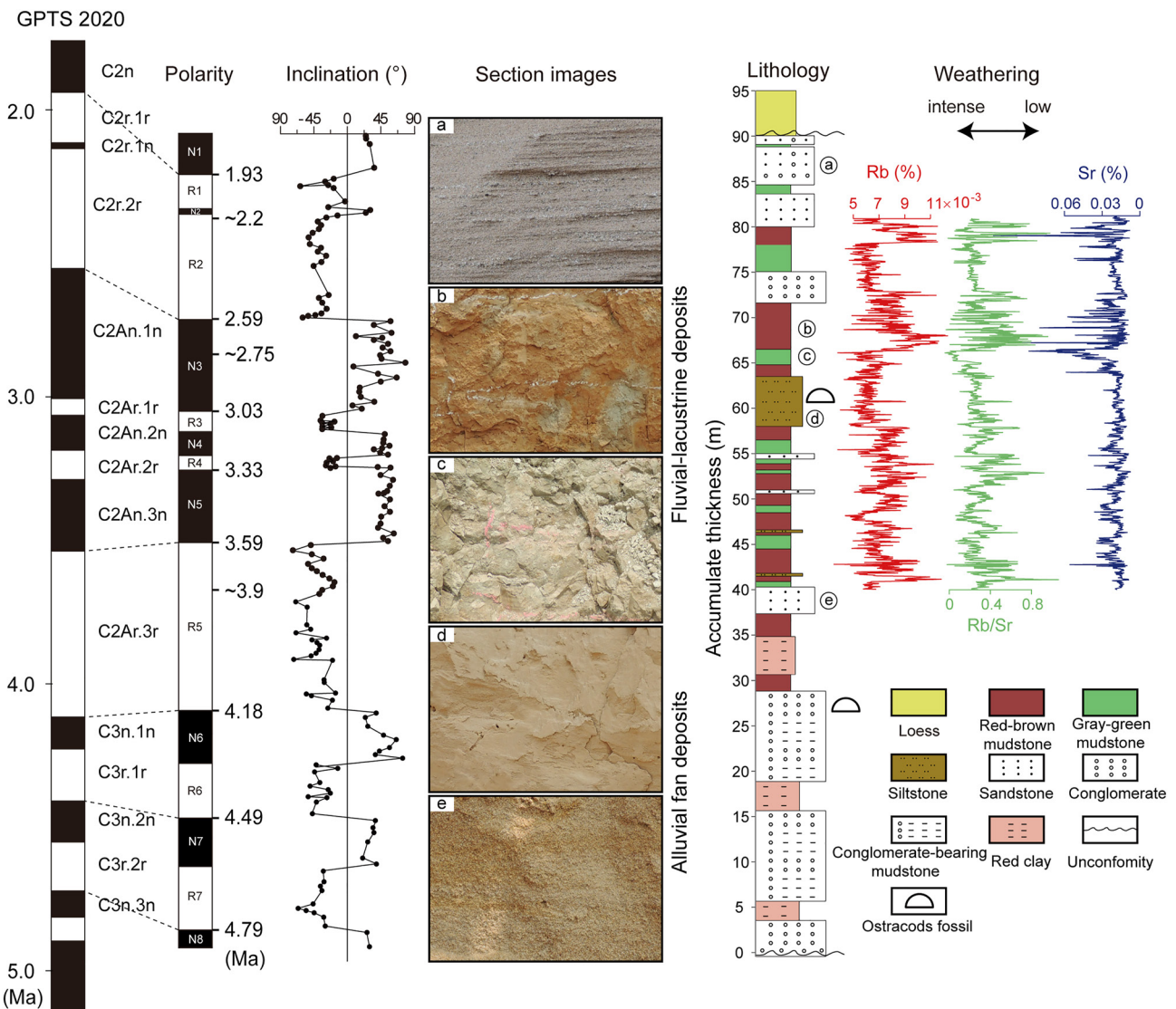


**Figure 1.** Regional lithostratigraphic and magnetostratigraphic correlations. Lithostratigraphy, magnetostratigraphy, Rb, Sr content and Rb/Sr ratios (40–81 m) of the Huangdigou section, with correlation with the 2020 geomagnetic polarity time scale (GPTS 2020; Ogg, 2020). Each polarity zone in the magnetic polarity stratigraphy is defined by at least two data points. Ostracod fossil information is from Yuan. (1986). Photo (a) is fluvial sandstone in the upper part of the section; (b, c) are reddish-brown and gray-green mudstones interpreted as lacustrine deposits; (d, e) are siltstones and sandstones interpreted as lacustrine deposits. The location of the photos is marked on the lithology column.

## 4. Discussion

### 4.1. Eccentricity Pacing of East Asian Monsoonal Intensity Before the Pleistocene

Previous studies conducted on the Huangdigou section have shown that the Fenwei Basin has been tectonically stable since the Pliocene, and that sediment provenance has been steady over the study interval with a dominant source from the North China Craton (Chen et al., 2021; Z. X. Wang et al., 2022; Zhang et al., 2021). Our high-resolution Rb/Sr record reflects lake level (lacustrine expansions and contractions) and are thus interpreted to reflect regional climatic changes in the absence of strong tectonic or geomorphic control(s) on lake evolution. Westerly derived moisture was likely not an important source of rainfall in Central and Northern China during Plio-Pleistocene because of the early shielding effect of North Tibetan uplift on the track of the Westerlies (An et al., 2001). Instead, multiple lines of evidence (i.e., pollen analysis, isotopic data on biomarkers and carbonates, climate simulations) corroborate a dominant monsoonal source for the rainfall in Central and Northern China during those times (H. Y. Lu et al., 2019; H. L. Wang et al., 2019). Our Rb/Sr record is thus interpreted as a direct

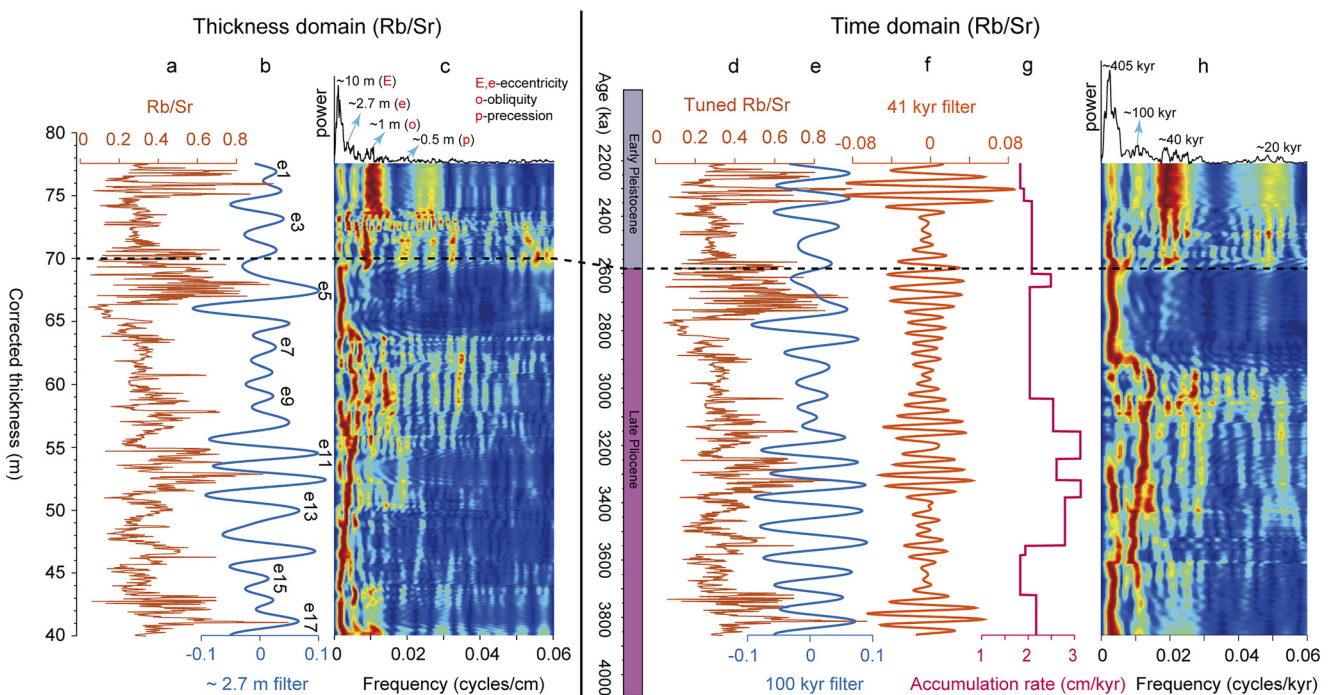


**Figure 2.** Cyclostratigraphic (astronomical) evolution in the thickness and time domain of the Sanmen paleolake from the Huangdigou section. (a) The Rb/Sr data in the 40–77.6 m (corrected thickness) interval are shown. (b) The Rb/Sr data band-pass filtered curves of 40–77.6 m ( $0.004 \pm 0.0024$  cycles/cm). (c) 2π-multitaper method evolutive Fast Fourier transform spectrogram using a 600 kyr sliding window shows variance in the Rb/Sr series in the thickness domain. (d) Floating Rb/Sr time series (after cyclostratigraphic calibration). (e) ~100 kyr filtered curve (Rb/Sr,  $0.01 \pm 0.003$  cycles/kyr). (f) ~41 kyr filtered curve (Rb/Sr,  $0.025 \pm 0.005$  cycles/kyr). (g) Estimated accumulation rate of Huangdigou section. (h) 2π-multitaper method evolutive Fast Fourier transform spectrogram using a 400 kyr sliding window shows variance in the Rb/Sr time series in the time domain. The black dashed line indicates the timing of a significant enhancement of the 41 kyr cycle.

proxy for changes in EASM intensity and penetration on orbital time scales (see Text S2 in Supporting Information S1 for a detailed explanation of climate proxies).

The influence of eccentricity on insolation is too weak to force monsoonal hydroclimate directly, but eccentricity can have an impact on regional insolation via its modulation of precession (S. C. Clemens & Tiedemann, 1997; Ruddiman, 2008). Nevertheless, the Rb/Sr data in our section show only very weakly developed precession cycles (Figure 2), as seen in many previous Tibetan records (Ao, Rohling, et al., 2021; Z. X. Wang et al., 2018, 2019). Precession forcing can transfer into the eccentricity band in sedimentary archives via mechanisms related to post-depositional diagenesis, stratal hiatuses and biological disturbance that are still poorly understood (e.g., Hilgen et al., 2015; Kemp, 2011; Ripepe & Fischer, 1991). Asymmetry in the response of proxies for past moisture to precession-band insolation forcing may also contribute to prominent eccentricity signal; this asymmetry has been proposed for magnetic susceptibility (MS), which may record faithfully intervals of increased rainfall while missing some intervals of decreased rainfall (Cheng et al., 2021; Sun, An, et al., 2010). This bias remains yet to be shown for Rb/Sr data. The over-expression of eccentricity might also reflect a non-linear monsoonal response to insolation forcing (e.g., S. C. Clemens et al., 2018; Hilgen et al., 2015; Kemp, 2011; Ripepe & Fischer, 1991). All mechanisms proposed to explain a strong eccentricity control on monsoonal intensity rely on non-linear amplification mechanisms related to Antarctic ice-sheet (AIS) dynamics, eustatic sea level and the global carbon cycle (Ao, Liebrand, et al., 2021; Nie et al., 2017; Z. X. Wang et al., 2019, 2021). AIS volume and eustatic sea-level are prominently forced by eccentricity for most of the Oligocene-Miocene (De Boer et al., 2014; Holbourn et al., 2013; Pälike et al., 2006).

Three amplification mechanisms have been proposed to relate EASM intensity, eustatic sea-level and AIS growth. (a) Periodic advances and retreats of East Asian coastlines related to eustatic variations forced by periodic changes in AIS size could impact moisture availability along the pathway of EASM winds (Nie et al., 2017); (b) Periodic AIS expansions could impact the Pacific meridional overturning circulation and Pacific sea surface temperature (SST) gradients, which affect the cross-equatorial pressure/heat gradient and the amount of regional latent heat,

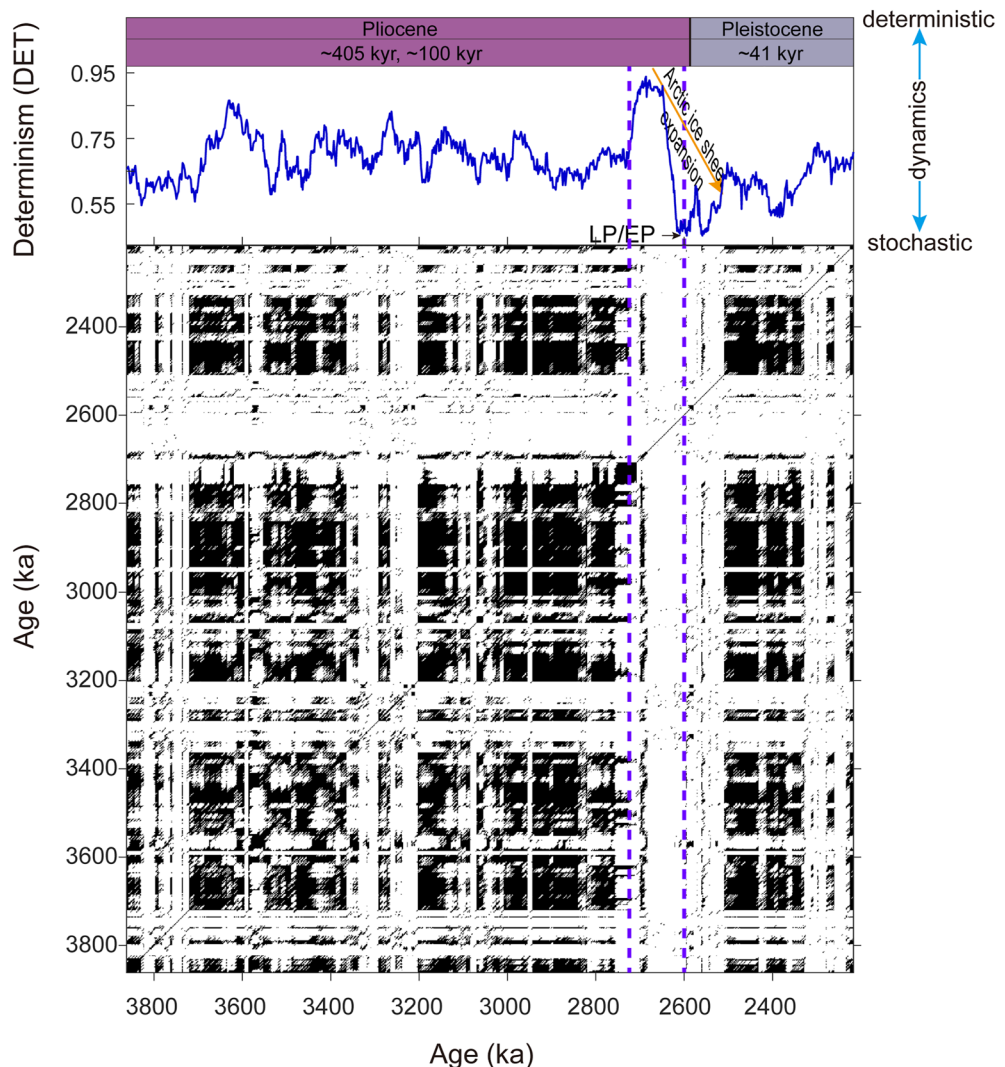


**Figure 3.** Recurrence plot and determinism (DET) values of Rb/Sr in the Sanmenxia Basin. A transition in recurrence plot from darker areas before ~2.75 Ma to white areas afterward indicate a prominent system change (e.g., see Marwan et al., 2007). Recurrence analysis of determinism (DET) shows that climate in warmer intervals is generally more deterministic (predictable) than in cooler intervals. From 3.9 Ma toward the LP/EP at 2.75 Ma determinism rises, approaching a threshold in the climate system (peak DET), DET values stabilized at a low level after 2.6 Ma.

modulating EASM moisture transport (Ao, Liebrand, et al., 2021; Nie et al., 2017); (c) AIS expansions could impact the Atlantic meridional overturning circulation and Atlantic SST gradients, which influences the strength and position of westerly winds; they in turn could have controlled the supply of westerly derived moisture during Miocene times (Z. X. Wang et al., 2019) and/or the penetration of the EASM (Ao, Liebrand, et al., 2021).

To better understand the links between EASM intensity and global climate changes, we reconstructed meridional SST gradients through the studied interval (Text S7; Figure S5 in Supporting Information S1). Meridional SST gradients increased over the period 2.75–2.6 Ma (Figures 4d and 4e) and shifted from dominant ~100 kyr eccentricity to ~41 kyr obliquity cycles (Figure S6 in Supporting Information S1). In our record, this time window corresponds to (a) a peak of DET values; (b) the disappearance of 100 kyr cyclicity; (c) a peak in Rb/Sr values (Figure 4). The synchronicity between our record and meridional SST gradients over this period supports a genetic relationship between the global overturning circulation and EASM intensity. However, phase analysis indicates a nearly 90° lag (~25 kyr) between these different records (Figures S6c and S6d in Supporting Information S1). We thus suggest that late Pliocene changes in meridional SST gradients might not have been the only cause of the shift in EASM sensitivity.

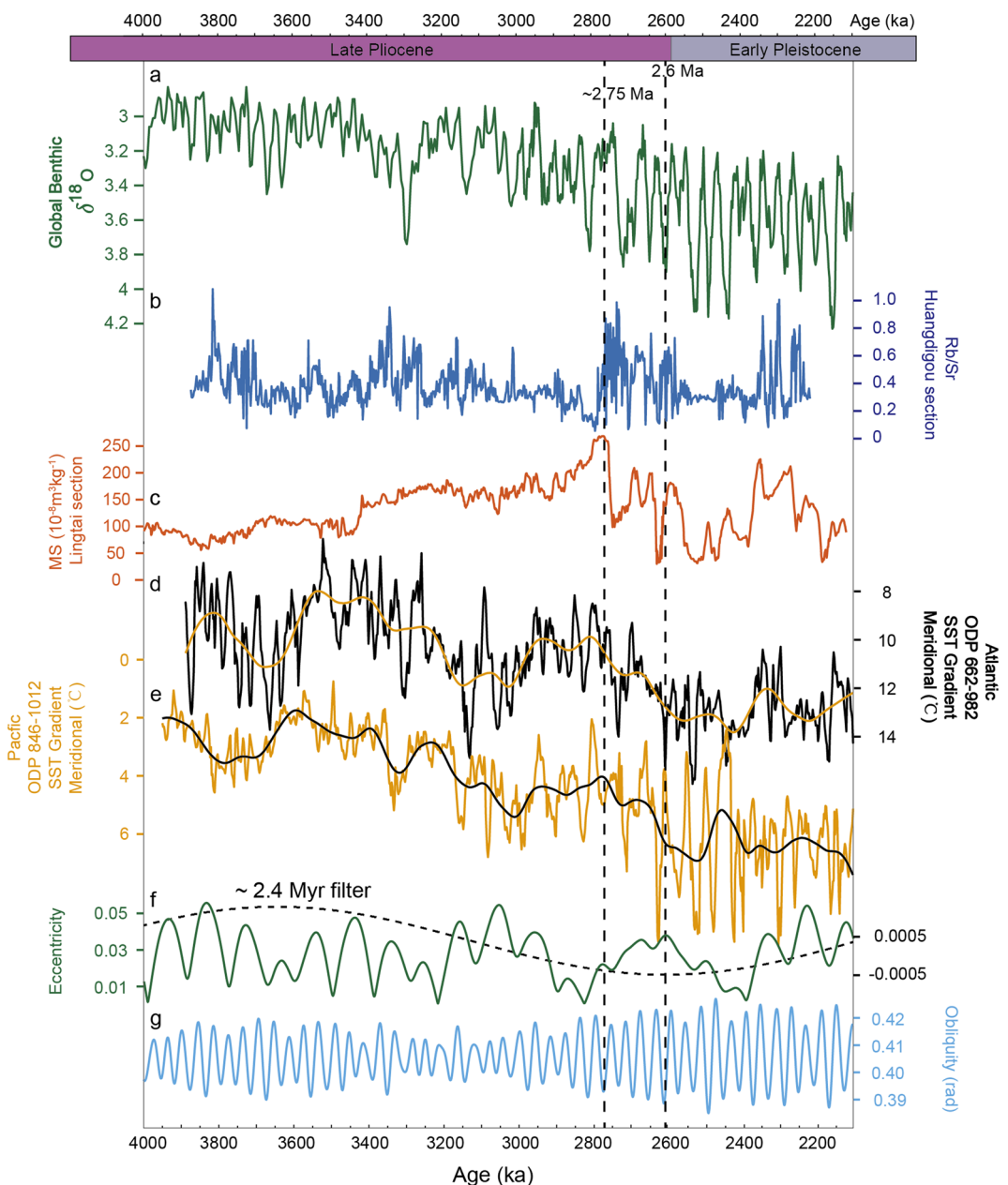


**Figure 4.** Terrestrial climate changes of the Sanmenxia Basin and China Loess Plateau and comparison with benthic  $\delta^{18}\text{O}$ , Atlantic meridional sea surface temperature (SST) gradient and Pacific meridional SST gradient across the LP/EP transition. (a) Global Benthic  $\delta^{18}\text{O}$  from the global compilation (LR04 stack; Lisiecki & Raymo, 2005). (b) Rb/Sr of the Huangdigou section in the Sanmenxia Basin. (c) Magnetic susceptibility of the Lingtai section in the China Loess Plateau (Sun et al., 2010). (d) Meridional SST gradient between Ocean Drilling Program (ODP) Sites 982 and 662 (Atlantic; K. Lawrence et al., 2009; Herbert et al., 2010). The orange line is obtained using a 200 kyr running mean. (e) Meridional SST gradient between ODP Sites 846 and 1,012 (Pacific; Z. Liu & Herbert, 2004; K. T. Lawrence et al., 2006; C. M. Brierley et al., 2009). The black line is obtained using a 200 kyr running mean. (f) The La2004 eccentricity solution (Laskar et al., 2004). The black dashed line is the ~2.4 Myr filtered curve (eccentricity,  $0.00042 \pm 0.00015$  cycles/kyr). (g) The La2004 obliquity solution (Laskar et al., 2004).

#### 4.2. Response of Northern Hemispheric Ice Sheet Expansion to Obliquity-Forcing Climate Change in East Asian Across the Pliocene-Pleistocene Transition

Our record bridges the gap between Mio-Pliocene lacustrine records, which show a climatic sensitivity to eccentricity forcing in NE Tibet (Ao, Liebrand, et al., 2021; Ao, Rohling, et al., 2021; Nie et al., 2017; Z. X. Wang

et al., 2018, 2019, 2021; Figure S3 in Supporting Information S1), and Pleistocene records that show more regional and temporal complexity and more prominent obliquity forcing (T. Li et al., 2017; Sun, An, et al., 2010). The shift to a more prominent obliquity signal after the 2.75–2.6 Ma interval is also corroborated by several other (non lacustrine) East Asian records. Notably, obliquity forcing significantly increases in MS records from Chinese loess-paleosol sequences at 2.75–2.59 Ma (Sun, Clemens, et al., 2006, 2010). Spectral analysis of previously published carbonate content data in the Plio-Pleistocene elolian Red Clay at the Lantian section (K. X. Wang et al., 2022; western part of Fenwei Basin) also shows a very similar evolution, with a prevalence of obliquity after 2.6 Ma (Figure S4 in Supporting Information S1), corroborating the regional nature of the observed change.

Eccentricity forcing of AIS volume and eustatic sea-level was prominent for most of the Pliocene until obliquity forcing took over from eccentricity in driving AIS and eustatic sea-level dynamics at 2.9–2.6 Ma (De Boer et al., 2014). The 2.9–2.6 Ma time interval is coeval with the end of the mid-Pliocene warming event and the first major intensification of the Northern Hemisphere glaciation (NHG). This event is seen in North Atlantic climate proxy data, including deep-sea oxygen isotopes (M. E. Raymo et al., 1992), planktonic foraminiferal assemblages (Dowsett & Poore, 1990) and ice rafted debris abundance (Smith et al., 2018). The increased expression of obliquity in AIS and eustatic sea-level after ~2.9 Ma is attributed to a significant influence of obliquity on NHG growth, which in turn impacts AIS expansion via eustatic feedback (De Boer et al., 2014). The change of orbital forcing in our Plio-Pleistocene record at 2.6 Ma is similar with the changes in AIS and eustatic orbital forcing. Our results thus suggest strong teleconnections between AIS expansion, eustatic sea level and EASM intensity.

DET values highlight that the change in orbital forcing after 2.75–2.6 Ma was associated with a shift to a more stochastic monsoonal response to NHG (Figure 3). The marked rise in DET values during the 2.75–2.7 Ma interval suggests the crossing of a tipping point in monsoonal dynamics (Scheffer et al., 2009; Westerhold et al., 2020). Recurrence analysis of the South Asian summer monsoon recorded by grain size in the Arabian Sea Ocean Drilling Program Site 722 (S. C. Clemens et al., 2008) shows a similar trend (Figure S7 in Supporting Information S1). These results suggest that the changes in Asian climate stochasticity across the Plio-Pleistocene boundary also affected the South Asian monsoon. We attribute this shift to the influence of NHG on central and East Asian climate. The shift is followed ~400 kyr later by a major transition in global climate state seen in global benthic  $\delta^{18}\text{O}$  and  $\delta^{13}\text{C}$  recurrence plots (transition from “coolhouse” to “icehouse”; Westerhold et al., 2020). This ~400 kyr delay suggests that NHG onset impacted the global carbon cycle and monsoonal intensity in different ways and that global temperatures were likely not the direct driver of the change in monsoonal sensitivity (Y. C. Wang et al., 2020). NHG ice and low temperatures at high northern latitudes have been shown to impact EASM intensity by influencing the strength of the Siberian high (Gai et al., 2020; Guo et al., 2004), the locus of the westerly track (Abell et al., 2021), meridional shift of the intertropical convergence zone (Haug et al., 2001; Yancheva et al., 2007) and changes in SST gradients (C. M. Brierley & Fedorov, 2010). The diversity of these potential forcing mechanisms can partly explain the regional, temporal, and proxy-related orbital complexity seen in late Pleistocene EASM records (Gai et al., 2020; T. Li et al., 2017; Sun, Kutzbach, et al., 2015). We postulate that their combination results in the increased stochasticity seen in our record.

If the large-scale features of the EASM were mainly constrained by Asian geography and topography and were roughly steady over the last 40 Ma (Farnsworth et al., 2019; Licht et al., 2016), our results indicate that polar glaciations significantly impacted the EASM circulation. It is noteworthy that the extra-long (~2.4 Myr) eccentricity cycle is close to a minimum between 2.75 and 2.6 Ma (Figures 4f and 4g). This orbital configuration indicates a significant weakening of Northern Hemisphere seasonality, promoting ice sheet growth at this time (E. Raymo & Nisancioglu, 2003), and the appearance of cool summers may also account for the significant weakening of the Asian summer monsoon. The EASM was similarly affected during the AIS expansion across the Eocene-Oligocene Transition (EOT; Ao, Dupont-Nivet, et al., 2020). A recurrence analysis of low frequency MS ( $\chi_{lf}$ ) data, an indicator of EASM intensity (Ao, Dupont-Nivet, et al., 2020; C. Y. Liu et al., 2021; Sun, Clemens, et al., 2006), from the lacustrine beds of the Lanzhou Basin across the EOT (Ao, Dupont-Nivet, et al., 2020), shows that DET values peaked at 34 Ma and gradually decreased across the early Oligocene glaciation (Figure S8 in Supporting Information S1). Thus, polar ice sheets appear to have played a crucial role in determining EASM variability on orbital time-scales. Quaternary monsoons likely display a sensitivity that is unique to the modern icehouse with bipolar ice sheets. These results call for caution when using Miocene coolhouse records or earlier warmhouse archives as analogs to predict monsoonal responses to global warming.

## 5. Conclusions

Our geochemical data from the Sanmenxia Basin highlight a major shift from eccentricity forcing to obliquity forcing of hydroclimate across the Plio-Pleistocene transition (~2.6 Ma). This is also associated with an increase in climate stochasticity as indicated by recurrence analysis. Combined with previous cyclostratigraphic studies from NE Tibetan lakes, our new results show that the EASM was paced by eccentricity in a uni-polar ice-sheet configuration, and shifted to a 41 kyr obliquity response as soon as bipolar ice sheets emerged. Our findings emphasize that global boundary conditions are thus equally important as local low-latitude insolation forcing for the EASM.

## Data Availability Statement

All of our measured proxy data presented here available in the figshare website (available from <https://doi.org/10.4121/14820342>).

## Acknowledgments

This work was supported by the National Natural Science Foundation of China (No. 42230208; 42172039). We thank Norbert Marwan, Alexey Fedorov and Yalong Fu, who offered help for this study.

## References

- Abell, J. T., Winckler, G., Anderson, R. F., & Herbert, T. D. (2021). Poleward and weakened westerlies during Pliocene warmth. *Nature*, 589(7840), 70–75. <https://doi.org/10.1038/s41586-020-03062-1>
- An, Z. S. (2000). The history and variability of the East Asian paleomonsoon climate. *Quaternary Science Reviews*, 19(1–5), 171–187. [https://doi.org/10.1016/s0277-3791\(99\)00060-8](https://doi.org/10.1016/s0277-3791(99)00060-8)
- An, Z. S., Kutzbach, J. E., Prell, W. L., & Porter, S. C. (2001). Evolution of Asian monsoons and phased uplift of the Himalaya-Tibetan plateau since Late Miocene times. *Nature*, 411(6833), 62–66. <https://doi.org/10.1038/35075035>
- Ao, H., Dupont-Nivet, G., Rohling, E. J., Zhang, P., Ladant, J. B., Roberts, A. P., et al. (2020). Orbital climate variability on the northeastern Tibetan Plateau across the Eocene-Oligocene transition. *Nature Communications*, 11, 1–11. <https://doi.org/10.1038/s41467-020-18824-8>
- Ao, H., Liebrand, D., Dekkers, M. J., Zhang, P., Song, Y., Liu, Q., et al. (2021). Eccentricity-paced monsoon variability on the northeastern Tibetan Plateau in the Late Oligocene high CO<sub>2</sub> world. *Science Advances*, 7(51), eabk2318. <https://doi.org/10.1126/sciadv.abk2318>
- Ao, H., Rohling, E. J., Zhang, R., Roberts, A. P., Holbourn, A. E., Ladant, J. B., et al. (2021). Global warming-induced Asian hydrological climate transition across the Miocene-Pliocene boundary. *Nature Communications*, 12, 1–13. <https://doi.org/10.1038/s41467-021-27054-5>
- Brierley, C. M., & Fedorov, A. V. (2010). Relative importance of meridional and zonal sea surface temperature gradients for the onset of the ice ages and Pliocene-Pleistocene climate evolution. *Paleoceanography*, 25(2), 2214. <https://doi.org/10.1029/2009pa001809>
- Brierley, C. M., Fedorov, A. V., Liu, Z., Herbert, T. D., Lawrence, K. T., & LaRiviere, J. P. (2009). Greatly expanded tropical warm pool and weakened Hadley circulation in the early Pliocene. *Science*, 323(5922), 1714–1718. <https://doi.org/10.1126/science.1167625>
- Chen, X. Q., Dong, S., Shi, W., Zuza, A. V., Li, Z., Chen, P., et al. (2021). Magnetostratigraphic ages of the Cenozoic Weihe and Shanxi Grabens in North China and their tectonic implications. *Tectonophysics*, 813, 228914. <https://doi.org/10.1016/j.tecto.2021.228914>
- Cheng, H., Zhang, H., Cai, Y., Shi, Z., Yi, L., Deng, C., et al. (2021). Orbital-scale Asian summer monsoon variations: Paradox and exploration. *Science China Earth Sciences*, 64(4), 529–544. <https://doi.org/10.1007/s11430-020-9720-y>
- Clemens, S. C., Holbourn, A., Kubota, Y., Lee, K. E., Liu, Z., Chen, G., et al. (2018). Precession-band variance missing from East Asian monsoon runoff. *Nature Communications*, 9(1), 3364. <https://doi.org/10.1038/s41467-018-05814-0>
- Clemens, S. C., Prell, W. L., Sun, Y., Liu, Z., & Chen, G. (2008). Southern hemisphere forcing of Pliocene δ<sup>18</sup>O and the evolution of Indo-Asian monsoons. *Paleoceanography*, 23(4). <https://doi.org/10.1029/2008pa001638>
- Clemens, S. C., & Tiedemann, R. (1997). Eccentricity forcing of Pliocene–early Pleistocene climate revealed in a marine oxygen-isotope record. *Nature*, 385(6619), 801–804. <https://doi.org/10.1038/385801a0>
- De Boer, B., Lourens, L. J., & van de Wal, R. S. W. (2014). Persistent 400, 000-year variability of Antarctic ice volume and the carbon cycle is revealed throughout the Plio-Pleistocene. *Nature Communications*, 5, 1–8.
- De Vleeschouwer, D., Drury, A. J., Vahlenkamp, M., Rochholz, F., Liebrand, D., & Palike, H. (2020). High-latitude biomes and rock weathering mediate climate-carbon cycle feedbacks on eccentricity timescales. *Nature Communications*, 11(1), 5013. <https://doi.org/10.1038/s41467-020-18733-w>
- Dowsett, H. J., & Poore, R. Z. (1990). A new planktic foraminifer transfer function for estimating Pliocene through Holocene sea surface temperatures. *Marine Micropaleontology*, 16(1–2), 1–23. [https://doi.org/10.1016/0377-8398\(90\)90026-i](https://doi.org/10.1016/0377-8398(90)90026-i)
- Farnsworth, A., Lunt, D. J., Robinson, S. A., Valdes, P. J., Roberts, W. H. G., Clift, P. D., et al. (2019). Past East Asian monsoon evolution controlled by paleogeography, not CO<sub>2</sub>. *Science Advances*, 5(10), eaax1697. <https://doi.org/10.1126/sciadv.aax1697>
- Gai, C. C., Liu, Q., Roberts, A. P., Chou, Y., Zhao, X., Jiang, Z., & Liu, J. (2020). East Asian monsoon evolution since the late Miocene from the South China Sea. *Earth and Planetary Science Letters*, 530, 115960. <https://doi.org/10.1016/j.epsl.2019.115960>
- Guo, Z. T., Peng, S., Hao, Q., Biscaye, P. E., An, Z., & Liu, T. (2004). Late Miocene-Pliocene development of Asian aridification as recorded in the Red-Earth Formation in northern China. *Global and Planetary Change*, 41(3–4), 135–145. <https://doi.org/10.1016/j.gloplacha.2004.01.002>
- Haug, G. H., Hughen, K. A., Sigman, D. M., Peterson, L. C., & Rohl, U. (2001). Southward migration of the intertropical convergence zone through the Holocene. *Science*, 293(5533), 1304–1308. <https://doi.org/10.1126/science.1059725>
- Herbert, T., Peterson, L., Lawrence, K., & Liu, Z. (2010). Tropical ocean temperatures over the past 3.5 million years. *Science*, 328(5985), 1530–1534. <https://doi.org/10.1126/science.1185435>
- Hilgen, F. J., Hinnov, L. A., Abdul Aziz, H., Abels, H. A., Batenburg, S., Bosmans, J. H. C., et al. (2015). Stratigraphic continuity and fragmentary sedimentation: The success of cyclostratigraphy as part of integrated stratigraphy. *Geological Society, London, Special Publications*, 404(1), 157–197. <https://doi.org/10.1144/sp404.12>
- Holbourn, A., Kuhnt, W., Frank, M., & Haley, B. A. (2013). Changes in Pacific Ocean circulation following the Miocene onset of permanent Antarctic ice cover. *Earth and Planetary Science Letters*, 365, 38–50. <https://doi.org/10.1016/j.epsl.2013.01.020>
- Howell, P., Pisias, N., Ballance, J., Baughman, J., & Ochs, L. (2006). ARAND time-series analysis software. Brown University.
- Huang, W. B., & Ji, H. X. (1984). A brief of Quaternary mammalian fossils of the Sanmenxia district. *Vertebrata Palasiatica*, 22, 230–238.

- Huang, W. B., & Sun, C. Y. (1959). Field trip guide of the Quaternary geological symposium at Sanmenxia reservoir. In *Chinese society of quaternary sciences ed. Memoirs on Sanmenxia quaternary geological symposium* (pp. 141–146). Science Press.
- Jin, Z. D., Yu, J. M., Zhang, F., & Qiang, X. K. (2020). Glacial-interglacial variation in catchment weathering and erosion paces the Indian summer monsoon during the Pleistocene. *Quaternary Science Reviews*, 248, 106619. <https://doi.org/10.1016/j.quascirev.2020.106619>
- Kemp, D. B. (2011). Shallow-water records of astronomical forcing and the eccentricity paradox. *Geology*, 39(5), 491–494. <https://doi.org/10.1130/g31878.1>
- Kripalani, R. H., Oh, J. H., & Chaudhari, H. S. (2007). Response of the East Asian summer monsoon to doubled atmospheric CO<sub>2</sub>: Coupled climate model simulations and projections under IPCC AR4. *Theoretical and Applied Climatology*, 87(1–4), 1–28. <https://doi.org/10.1007/s00704-006-0238-4>
- Laskar, J., Robutel, P., Joutel, F., Gastineau, M., Correia, A. C. M., & Levrard, B. (2004). A long-term numerical solution for the insolation quantities of the Earth. *Astronomy & Astrophysics*, 428(1), 261–285. <https://doi.org/10.1051/0004-6361:20041335>
- Lawrence, K., Herbert, T., Brown, C., Raymo, M., & Haywood, A. (2009). High amplitude variations in North Atlantic Sea surface temperature during the early Pliocene warm period. *Paleoceanography*, 24(2), 2218. <https://doi.org/10.1029/2008pa001669>
- Lawrence, K. T., Liu, Z. H., & Herbert, T. D. (2006). Evolution of the eastern tropical Pacific through Plio-Pleistocene glaciation. *Science*, 312(5770), 79–83. <https://doi.org/10.1126/science.1120395>
- Li, M. S., Hinov, L., & Kump, L. (2019). Acycle: Time-series analysis software for paleoclimate research and education. *Computers & Geosciences*, 127, 12–22. <https://doi.org/10.1016/j.cageo.2019.02.011>
- Li, T., Liu, F., Abels, H. A., You, C. F., Zhang, Z., Chen, J., et al. (2017). Continued obliquity pacing of East Asian summer precipitation after the mid-Pleistocene transition. *Earth and Planetary Science Letters*, 457, 181–190. <https://doi.org/10.1016/j.epsl.2016.09.045>
- Licht, A., Dupont-Nivet, G., Pullen, A., Kapp, P., Abels, H. A., Lai, Z., et al. (2016). Resilience of the Asian atmospheric circulation shown by Paleogene dust provenance. *Nature Communications*, 7, 1–6. <https://doi.org/10.1038/ncomms12390>
- Lisiecki, L. E., & Raymo, M. E. (2005). A Pliocene-Pleistocene stack of 57 globally distributed benthic δ<sup>18</sup>O records. *Paleoceanography*, 20(1), 1003. <https://doi.org/10.1029/2004pa001071>
- Liu, C. Y., Nie, J., Li, Z., Qiao, Q., Abell, J. T., Wang, F., & Xiao, W. (2021). Eccentricity forcing of East Asian monsoonal systems over the past 3 million years. *Proceedings of the National Academy of Sciences of the United States of America*, 118(43). <https://doi.org/10.1073/pnas.2107055118>
- Liu, J., Chen, X., Shi, W., Chen, P., Zhang, Y., Hu, J., et al. (2019). Tectonically controlled evolution of the Yellow River drainage system in the Weihe region, North China: Constraints from sedimentation, mineralogy and geochemistry. *Journal of Asian Earth Sciences*, 179, 350–364. <https://doi.org/10.1016/j.jseas.2019.05.008>
- Liu, J. B., Chen, J., Zhang, X., Li, Y., Rao, Z., & Chen, F. (2015). Holocene East Asian summer monsoon records in northern China and their inconsistency with Chinese stalagmite δ<sup>18</sup>O records. *Earth-Science Reviews*, 148, 194–220. <https://doi.org/10.1016/j.earscirev.2015.06.004>
- Liu, Z., & Herbert, T. D. (2004). High-latitude influence on the eastern equatorial Pacific climate in the early Pleistocene epoch. *Nature*, 427(6976), 720–723. <https://doi.org/10.1038/nature02338>
- Lu, H., Yi, S., Liu, Z., Mason, J. A., Jiang, D., Cheng, J., et al. (2013). Variation of East Asian monsoon precipitation during the past 21 ky and potential CO<sub>2</sub> forcing. *Geology*, 41(9), 1023–1026. <https://doi.org/10.1130/g34488.1>
- Lu, H. Y., Wang, X., Wang, X., Chang, X., Zhang, H., Xu, Z., et al. (2019). Formation and evolution of Gobi Desert in central and eastern Asia. *Earth-Science Reviews*, 194, 251–263. <https://doi.org/10.1016/j.earscirev.2019.04.014>
- Lu, J. Y., Yang, H., Griffiths, M. L., Burls, N. J., Xiao, G., Yang, J., et al. (2021). Asian monsoon evolution linked to Pacific temperature gradients since the Late Miocene. *Earth and Planetary Science Letters*, 563, 116882. <https://doi.org/10.1016/j.epsl.2021.116882>
- Luo, Z., Nie, J., Moe, A. E., Heerman, R. V., Garzione, C., Herbert, T. D., et al. (2021). Joint insolation and ice sheet/CO<sub>2</sub> forcing on northern China precipitation during Pliocene warmth. *Science Bulletin*, 66(4), 319–322. <https://doi.org/10.1016/j.scib.2020.10.025>
- Marwan, N., Romano, M. C., Thiel, M., & Kurths, J. (2007). Recurrence plots for the analysis of complex systems. *Physics Reports*, 438(5–6), 237–329. <https://doi.org/10.1016/j.physrep.2006.11.001>
- Nie, J. S., Garzione, C., Su, Q., Liu, Q., Zhang, R., Heslop, D., et al. (2017). Dominant 100, 000-year precipitation cyclicity in a late Miocene lake from northeast Tibet. *Science Advances*, 3, e1600762. <https://doi.org/10.1126/sciadv.1600762>
- Ogg, J. G. (2020). Geomagnetic polarity time scale. In *Geologic time scale 2020* (pp. 159–192).
- Páliké, H., Fraizer, J., & Zachos, J. C. (2006). Extended orbitally forced palaeoclimatic records from the equatorial Atlantic Ceara Rise. *Quaternary Science Reviews*, 25(23–24), 3138–3149. <https://doi.org/10.1016/j.quascirev.2006.02.011>
- Raymo, E., & Nisancioglu, K. H. (2003). The 41 kyr world: Milankovitch's other unsolved mystery. *Paleoceanography*, 18(1), 1011. <https://doi.org/10.1029/2002pa000791>
- Raymo, M. E., Hodell, D., & Jansen, E. (1992). Response of deep ocean circulation to initiation of Northern Hemisphere glaciation (3–2 Ma). *Paleoceanography*, 7(5), 645–672. <https://doi.org/10.1029/92pa01609>
- Ripepe, M., & Fischer, A. G. (1991). Stratigraphic rhythms synthesized from orbital variations. In E. K. Franseen, W. Lynn Watney, G. Christopher St Kendall, & W. Ross (Eds.), *Sedimentary modeling: Computer simulations and methods for improved parameter definition: Kansas state geological survey bulletin* (Vol. 233, pp. 335–344).
- Ruddiman, W. F. (2008). *Earth's climate: Past and future* (2nd ed.). W. H. Freeman and Company.
- Scheffer, M., Bascompte, J., Brock, W. A., Brovkin, V., Carpenter, S. R., Dakos, V., et al. (2009). Early-warning signals for critical transitions. *Nature*, 461(7260), 53–59. <https://doi.org/10.1038/nature08227>
- Smith, Y. M., Hill, D. J., Dolan, A. M., Haywood, A. M., Dowsett, H. J., & Risebrobakken, B. (2018). Icebergs in the Nordic seas throughout the late Pliocene. *Paleoceanography and Paleoclimatology*, 33(3), 318–335. <https://doi.org/10.1002/2017pa003240>
- Steffen, W., Rockström, J., Richardson, K., Lenton, T. M., Schellnhuber, H. J., Liverman, D., et al. (2018). Trajectories of the Earth system in the Anthropocene. *Proceedings of the National Academy of Sciences of the United States of America*, 115(33), 8252–8259. <https://doi.org/10.1073/pnas.1810141115>
- Sun, Y. B., An, Z. S., Clemens, S. C., Bloemendal, J., & Vandenberghe, J. (2010). Seven million years of wind and precipitation variability on the Chinese Loess Plateau. *Earth and Planetary Science Letters*, 297(3–4), 525–535. <https://doi.org/10.1016/j.epsl.2010.07.004>
- Sun, Y. B., Clemens, S. C., An, Z. S., & Yu, Z. W. (2006). Astronomical timescale and palaeoclimatic implication of stacked 3.6-Myr monsoon records from the Chinese Loess Plateau. *Quaternary Science Reviews*, 25(1–2), 33–48. <https://doi.org/10.1016/j.quascirev.2005.07.005>
- Sun, Y. B., Kutzbach, J., An, Z., Clemens, S., Liu, Z., Liu, W., et al. (2015). Astronomical and glacial forcing of East Asian summer monsoon variability. *Quaternary Science Reviews*, 115, 132–142. <https://doi.org/10.1016/j.quascirev.2015.03.009>
- Wang, B., Zheng, H. B., Wang, P., & He, Z. (2013). The cenozoic strata and depositional evolution of Weihe Basin: Progresses and problems. *Advances in Earth Science*, 28, 1126–1135.

- Wang, H. L., Lu, H., Zhao, L., Zhang, H., Lei, F., & Wang, Y. (2019). Asian monsoon rainfall variation during the Pliocene forced by global temperature change. *Nature Communications*, 10, 1–8. <https://doi.org/10.1038/s41467-019-13338-4>
- Wang, K. X., Lu, H., Garzione, C. N., Zhao, L., Liang, C., Li, S., et al. (2022). Enhanced soil respiration, vegetation and monsoon precipitation at Lantian, East Asia during Pliocene warmth. *Climate Dynamics*, 59(9–10), 1–15. <https://doi.org/10.1007/s00382-022-06243-y>
- Wang, S. B., Jiang, F. C., Wu, X. H., Wang, S. M., & Tian, G. Q. (2004). The connotation and significance of Sanmen formation. *Quaternary Sciences*, 24, 116–123.
- Wang, S. B., Jiang, F. C., Wu, X. H., Wang, S. M., Tian, G. Q., Xue, B., & Zheng, H. B. (1999). A study on the age of Sanmen group in Sammennexia area. *Journal of Geomechanics*, 5(4), 59–67.
- Wang, Y. C., Lu, H., Wang, K., Li, Y., & Clemens, S. (2020). Combined high-and low-latitude forcing of East Asian monsoon precipitation variability in the Pliocene warm period. *Science Advances*, 6(46), eabc2414. <https://doi.org/10.1126/sciadv.abc2414>
- Wang, Z. X., Huang, C. J., Licht, A., Zhang, R., & Kemp, D. B. (2019). Middle to late Miocene eccentricity forcing on lake expansion in NE Tibet. *Geophysical Research Letters*, 46(12), 6926–6935. <https://doi.org/10.1029/2019gl082283>
- Wang, Z. X., Mao, Y., Geng, J., Huang, C., Ogg, J., Kemp, D. B., et al. (2022). Pliocene-Pleistocene evolution of the lower Yellow River in eastern North China: Constraints on the age of the Sanmen gorge connection. *Global and Planetary Change*, 213, 103835. <https://doi.org/10.1016/j.gloplacha.2022.103835>
- Wang, Z. X., Shen, Y. J., Licht, A., & Huang, C. J. (2018). Cyclostratigraphy and magnetostratigraphy of the Middle Miocene Ashigong Formation, Guide Basin, China, and its implications for the paleoclimatic evolution of NE Tibet. *Paleoceanography and Paleoclimatology*, 33(10), 1066–1085. <https://doi.org/10.1029/2018pa003409>
- Wang, Z. X., Zhang, Z., Huang, C., Shen, J., Sui, Y., & Qian, Z. (2021). Astronomical forcing of lake evolution in the Lanzhou Basin during early Miocene period. *Earth and Planetary Science Letters*, 554, 116648. <https://doi.org/10.1016/j.epsl.2020.116648>
- Westerhold, T., Marwan, N., Drury, A. J., Liebrand, D., Agnini, C., Anagnostou, E., et al. (2020). An astronomically dated record of Earth's climate and its predictability over the last 66 million years. *Science*, 369(6509), 1383–1387. <https://doi.org/10.1126/science.aba6853>
- Xiao, G. Q., Pan, Q., Zhao, Q., Yin, Q., Chen, R., Ao, H., et al. (2021). Early Pleistocene integration of the Yellow River II: Evidence from the Plio-Pleistocene sedimentary record of the Fenwei Basin. *Palaeogeography, Palaeoclimatology, Palaeoecology*, 577, 110550. <https://doi.org/10.1016/j.palaeo.2021.110550>
- Yancheva, G., Nowaczyk, N. R., Mingram, J., Dulski, P., Schettler, G., Negendank, J. F. W., et al. (2007). Influence of the intertropical convergence zone on the East Asian monsoon. *Nature*, 445(7123), 74–77. <https://doi.org/10.1038/nature05431>
- Yuan, F. T. (1986). Discovery of ostracods from the Sanmen series and its significance. *Acta Micropalaeontologica Sinica*, 3, 161–167.
- Zhang, H., Lu, H., Zhou, Y., Cui, Y., He, J., Lv, H., et al. (2021). Heavy mineral assemblages and U-Pb detrital zircon geochronology of sediments from the Weihe and Sanmen Basins: New insights into the Pliocene-Pleistocene evolution of the Yellow River. *Palaeogeography, Palaeoclimatology, Palaeoecology*, 562, 110072. <https://doi.org/10.1016/j.palaeo.2020.110072>

## References From the Supporting Information

- Abels, H. A., Dupont-Nivet, G., Xiao, G., Bosboom, R., & Krijgsman, W. (2011). Step-wise change of Asian interior climate preceding the Eocene–Oligocene Transition (EOT). *Palaeogeography, Palaeoclimatology, Palaeoecology*, 299(3–4), 399–412. <https://doi.org/10.1016/j.palaeo.2010.11.028>
- Chang, H., An, Z., Wu, F., Jin, Z., Liu, W., & Song, Y. (2013). A Rb/Sr record of the weathering response to environmental changes in westerly winds across the Tarim Basin in the late Miocene to the early Pleistocene. *Palaeogeography, Palaeoclimatology, Palaeoecology*, 386, 364–373. <https://doi.org/10.1016/j.palaeo.2013.06.006>
- Dasch, E. J. (1969). Strontium isotopes in weathering profiles, deep-sea sediments, and sedimentary rocks. *Geochimica et Cosmochimica Acta*, 33(12), 1521–1552. [https://doi.org/10.1016/0016-7037\(69\)90153-7](https://doi.org/10.1016/0016-7037(69)90153-7)
- Dekens, P. S., Ravelo, A. C., McCarthy, M. D., & Edwards, C. A. (2008). A 5 million year comparison of Mg/Ca and alkenone paleothermometers. *Geochemistry, Geophysics, Geosystems*, 9(10). <https://doi.org/10.1029/2007gc001931>
- Eroglu, D., McRobie, F. H., Ozken, I., Stemler, T., Wyrwoll, K. H., Breitenbach, S. F. M., et al. (2016). See-saw relationship of the Holocene East Asian-Australian summer monsoon. *Nature Communications*, 7(1), 12929. <https://doi.org/10.1038/ncomms12929>
- Harvey, A. M., Mather, A. E., & Stokes, M. (2005). Alluvial fans: Geomorphology, sedimentology, dynamics—Introduction. A review of alluvial-fan research. In A. M. Harvey, A. E. Mather, & M. Stokes (Eds.), *Alluvial Fans: Geomorphology, sedimentology, dynamics*, (Vol. 251, pp. 1–7). Geological Society of London Special Publication.
- Jin, Z. D., Cao, J. J., Wu, J. L., & Wang, S. M. (2006). A Rb/Sr record of catchment weathering response to Holocene climate change in Inner Mongolia. *Earth Surface Processes and Landforms*, 31(3), 285–291. <https://doi.org/10.1002/esp.1243>
- Jones, C. H. (2002). User-driven integrated software lives: "Paleomag" paleomagnetics analysis on the Macintosh. *Computers & Geosciences*, 28(10), 1145–2115. [https://doi.org/10.1016/s0098-3004\(02\)00032-8](https://doi.org/10.1016/s0098-3004(02)00032-8)
- Mann, M. E., & Lees, J. M. (1996). Robust estimation of background noise and signal detection in climatic time series. *Climate Change*, 33(3), 409–445. <https://doi.org/10.1007/bf00142586>
- Marwan, N. (2020). Cross recurrence plot toolbox for MATLAB®, ver. 5.22 (R32.4). Retrieved from <http://tocsy.pik-potsdam.de/CRPtoolbox/accessed%202020-12-09>
- Meijer, N., Dupont-Nivet, G., Licht, A., Trabucho-Alexandre, J., Bourquin, S., & Abels, H. A. (2020). Identifying Eolian dust in the geological record. *Earth-Science Reviews*, 211, 103410. <https://doi.org/10.1016/j.earscirev.2020.103410>
- Schinkel, S., Dimigen, O., & Marwan, N. (2008). Selection of recurrence threshold for signal detection. *The European Physical Journal - Special Topics*, 164(1), 45–53. <https://doi.org/10.1140/epjst/e2008-00833-5>
- Weedon, G. P. (2003). Additional methods of time-series analysis. In S. Price (Ed.), *Time series analysis and cyclostratigraphy: Examining stratigraphic records of environmental cycles* (pp. 103–112). Cambridge University Press.